

Electronic Supplementary Information

Rhodium metallene supported platinum nanocrystals for ethylene glycol oxidation reaction

Yue Zhao^a, Zi-Han Yuan^a, Jiang-Tao Huang^b, Ming-Yao Wang^a, Bin He^{b*}, Yu Ding^a,
Pu-Jun Jin^a and Yu Chen^{a,*}

^a Key Laboratory of Macromolecular Science of Shaanxi Province, Shaanxi Key Laboratory for Advanced Energy Devices, Shaanxi Engineering Lab for Advanced Energy Technology, School of Materials Science and Engineering, Shaanxi Normal University, Xi'an 710062, PR China.

^b College of New Materials and New Energies, Shenzhen Technology University, Shenzhen, 518118, PR China.

* Corresponding authors

E-mail: hebin@sztu.edu.cn (B. He) and ndchenyu@gmail.com (Y. Chen)

1. Experimental section

1.1 Electrochemical measurements

All electrochemical tests were carried out on CHI-760 electrochemical analyzer at 30°C. In three-electrode system, a saturated calomel electrode was used as reference electrode, a carbon rod was served as the auxiliary electrode, an electrocatalyst-modified glassy carbon was used as working electrode. The electrocatalyst ink was achieved by dispersing 4 mg of the electrocatalyst in 2 mL of water. The 4 μL of the electrocatalyst ink was loaded onto the glassy carbon electrode surface and dried at room temperature. Then, 4 μL of Nafion solution (0.05wt %) was coated on the working electrode surface and dried at room temperature. The electrocatalyst loading mass density on working electrode was 114.3 $\mu\text{g cm}^{-2}$. All electrode potentials in this work were quoted versus the reversible hydrogen electrode (RHE).

1.2 Physical characterization

XRD tests were made on a DX-2700 X-ray diffractometer with Cu $K\alpha$ radiation source, Haoyuan Instrument Co., Ltd. SEM tests were carried out on a SU-8220 instrument, ITACHI. TEM images, SAED pattern, HAADF-STEM images, and HAADF-STEM-EDX-maps images were captured on TECNAI G2 F20 microscopy instrument, XPS spectra were achieved on an AXIS ULTRA spectrometer, Kratos Analytical.

1.3 DFT calculation

The interaction of the Rh and Pt atoms was calculated with DFT. All of the calculations were performed using the Materials Studio 7.0 Dmol3 program from Accelrys Software Inc. The exchange–correlation energy calculations were carried out with the generalized gradient approximation (GGA) within PW91. In the computational procedure, the DNP basis set and all-electron-core treatment were applied. The structure was fully optimized until the convergence criteria were as follows: the maximal force on the atoms was 0.004 Ha/Å, the maximal atomic displacement was 0.001 Å, the maximal energy change per atom was 1.0×10^{-5} eV, and the SCF convergence criterion was 1.0×10^{-4} . According to and our previous work, Pt (111) facets and Rh (111) facets are main facets as the model for calculation. DFT calculations of the adsorption energy at Pt/Rh(111) and Rh(111) were performed by Material studio within the local density approximation. The Brillouin zone was controlled within a $2 \times 2 \times 2$ Monkhorst–Pack grids. The optimized structure was obtained until the force on per atom is less than 10^{-4} eV/Å. To avoid the periodic interaction, a vacuum layer of 30 Å was added into the plate. The adsorption energy (ΔE_{ads}) was computed by $\Delta E_{\text{ads}} = E_{\text{M+N}} - E_{\text{M}} - E_{\text{N}}$, where E_{N} was the energy of CO in the gas phase, E_{M} was the energy of the clean metal surface, and $E_{\text{M+N}}$ was the optimized total energy of the system with CO species adsorbed on the metal surfaces.

2. Supplementary Figures

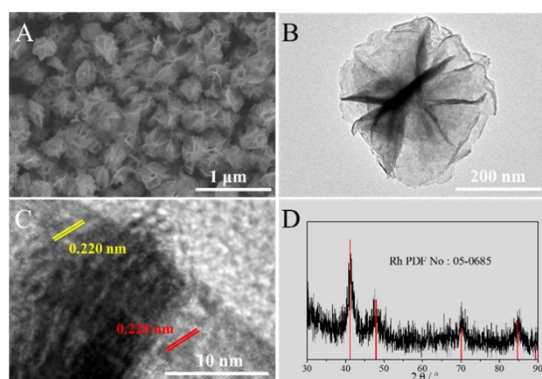


Fig. S1 (A) SEM image, (B) TEM image, (C) magnified TEM and (D) XRD pattern image of Rhlene.

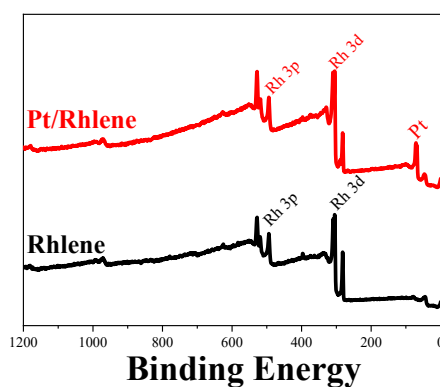


Fig. S2 XPS survey spectrum of Pt/Rhlene and Rhlene.

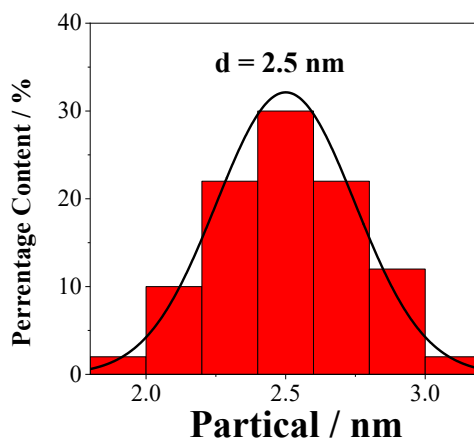


Fig. S3 Particle size distribution histogram of Pt nanoparticles at Pt/Rhlene.

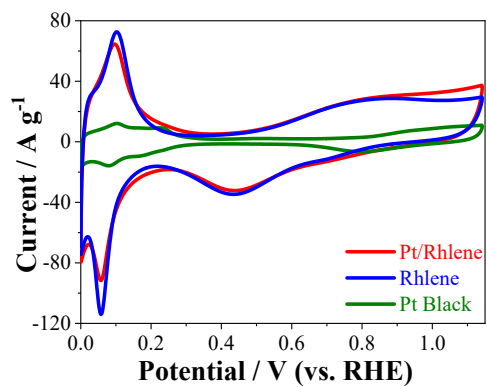


Fig. S4 CV curves of Pt/Rhylene, Rhylene, and Pt black in N_2 -purged 0.5 M H_2SO_4 solution at 5 mV s^{-1} .

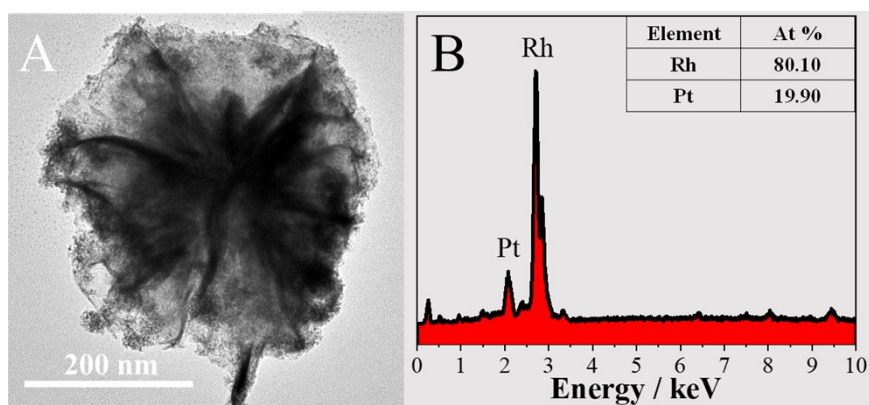


Fig. S5 (A) TEM pattern and (B) EDX spectrum of Pt/Rhylene after steady-state test.